

DAMAGE ESTIMATES FOR EUROPEAN AND U.S. SITES USING THE U.S. HIGH-CYCLE FATIGUE DATA BASE

Herbert J. Sutherland

Wind Energy Technology
Sandia National Laboratories
Albuquerque, NM 87185-0708
Phone: (505)844-2037
Fax: (505)845-9500
E-Mail: hjsuthe@sandia.gov

ABSTRACT

This paper uses two high-cycle fatigue data bases, one for typical U.S. blade materials and one for European materials, to analyze the service lifetime of a wind turbine blade subjected to the WISPER load spectrum for northern European sites [Ten Have, 1992] and the WISPER protocol load spectrum for U.S. wind farm sites [Kelley, 1995]. The U.S. data base, developed by Mandell, et al. (1995), contains over 2200 data points that were obtained using coupon testing procedures. These data are used to construct a Goodman diagram that is suitable for analyzing wind turbine blades. This result is compared to the Goodman diagram derived from the European fatigue data base FACT [DeSmet and Bach, 1994]. The LIFE2 fatigue analysis code for wind turbines [Sutherland and Schluter, 1989] is then used to predict the service lifetime of a turbine blade subjected to the two loading histories. The results of this study indicate that the WISPER load spectrum from northern European sites significantly underestimates the WISPER protocol load spectrum from a U.S. wind farm site; i.e., the WISPER load spectrum significantly underestimates the number and magnitude of the loads observed at a U.S. wind farm site. Further, the analyses demonstrate that the European and the U.S. fatigue material data bases are in general agreement for the prediction of tensile failures. However, for compressive failures, the two data bases are significantly different, with the U.S. data base predicting significantly shorter service lifetimes than the European data base.

INTRODUCTION

In recent papers, Mandell, et al. (1995), Samborsky and Mandell (1996) and Sutherland and Mandell (1996) have brought together the extensive set of S-N fatigue data that was developed at Montana State University (MSU) under the auspices of the U.S. DOE's Wind Energy Program. The data base, herein called the MSU/DOE data base, now contains over 2200 data points with test results for typical U.S. wind turbine blade materials, i.e., E-glass fiber composites with polyester, vinyl ester and epoxy matrices and with a variety of fiber contents and

architectures. Specimens were tested over a range of 10^3 to 5×10^8 cycles and at R values of 2, 10, -1, 0.5 and 0.1 (the R value is defined to be the algebraic ratio of the minimum stress σ_{\min} to the maximum stress σ_{\max} in one cycle). Supporting tests for ultimate tensile, ultimate compression, and modulus were also conducted for inclusion in the data base. The fatigue data are from constant-amplitude S-N tests that were conducted using conventional coupon test procedures and a specialized, high-speed coupon test procedure. The latter testing procedure was developed at MSU especially for these tests to permit high-cycle fatigue testing in a timely manner, see Mandell, et al. (1994).

Mandell, et al. (1993) have demonstrated that the data from the various fiberglass composite materials in the data base may be characterized by a power law curve fit when they are normalized to the ultimate tensile or compressive strength of the composite. Starting with the normalized curve fits at various R values, a Goodman diagram is constructed and then normalized to typical wind turbine blade properties. This normalization is required because the relatively small coupons in the data base perform significantly better than the relatively large composite structures used in typical blades.

To illustrate the use of these data, the Goodman diagram is used by the LIFE2 fatigue analysis code for wind turbines [Sutherland and Schluter, 1989] to analyze two distinct loading environments. The first is the Wind turbine reference SPEctRum, WISPER, herein called the European load spectrum, that was developed by Ten Have (1992) to be a loading standard that reproduces the general character of flap loads on a wind turbine blade. This load spectrum represents a more or less homogeneous view of the service environment seen by turbines operating individually in near-uniform terrain in the proximity to the ocean. The second load spectrum, herein called the U.S. wind farm load spectrum, was developed by Kelley (1995). In this formulation, the WISPER development protocol is applied to data from a California wind farm to obtain a load spectrum that is representative of the service environment for multi-row wind farms at continental sites dominated by complex terrain (i.e., mountain passes).

Fatigue analyses are used to compare the MSU/DOE fatigue characterization to the European data base FACT developed by DeSmet and Bach, (1994). Here, we demonstrate that the two data bases are in general agreement for tensile failure of the blade, but are significantly different in compression. Moreover, the MSU/DOE data base predicts the critical failure mode to be compressive, while the FACT data base predicts the mode to be tensile.

Fatigue analyses are also used to demonstrate the impact of the two operating environments on the predicted lifetime of the two characterizations. The analyses demonstrate that the WISPER load spectrum from northern European sites significantly underestimates the WISPER protocol load spectrum from a U.S. wind farm site; i.e., the WISPER load spectrum significantly underestimates the number and magnitude of the loads observed at a U.S. wind farm site.

MATERIAL CHARACTERIZATION

The MSU/DOE Data Base

The initial U.S. fatigue data base was reported by Mandell, Reed and Samborsky (1992). These data were obtained from constant-amplitude S-N tests using traditional coupon tests. The coupons were typically 25 to 50 mm (one to two inches) wide and 4 to 8 mm (an eighth to a quarter inch) thick. The internal hysteretic heating of these polymer-based materials, combined with their poor heat transfer characteristics, limited the testing frequency to below 20 Hz. Typically, these tests were run at a frequency of 10 Hz.

To cover the entire range of interest for wind turbine applications, the S-N data must extend to a minimum of 10^8 cycles. Using traditional techniques, one test would require over one hundred days to complete. Thus, an appropriate fatigue data base for wind turbine applications would be very difficult and time consuming to build when tests are limited to 10 or 20 Hz cyclic rates. To overcome this difficulty, Creed (1993) and Mandell, et al. (1994) developed a new testing technique that permits testing at frequencies up to 100 Hz, thus shortening the test period for 10^8 cycles to just eleven days. Adequate heat transfer is achieved in this technique by using relatively thin specimens, approximately 1.5 mm (0.06 inch) thick. This thickness limits the number of fiberglass layers to fewer than 10. Details of the test development and validation are discussed by Creed (1993) and Mandell, et al. (1995). The validation process included a detailed comparison of the S-N fatigue data produced using the relatively thin coupons to data produced using standard coupons. The comparison showed that the S-N data were within experimental scatter of one another.

As discussed by Sutherland and Mandell (1996), the data base now contains over 2200 data points with test results for E-glass fiber composites with polyester, vinyl ester and epoxy matrices. Many of the specimens used

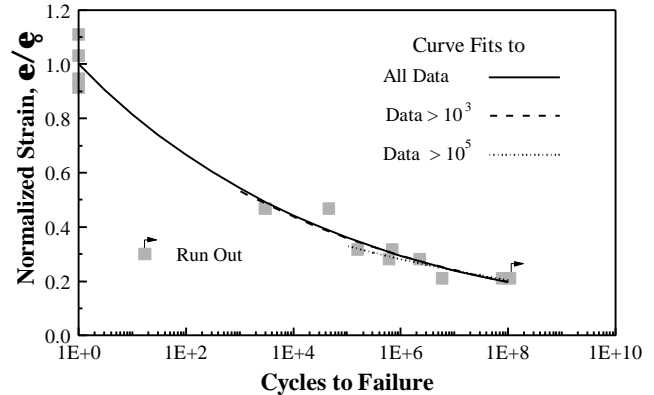


Figure 1. High cycle S-N data for R=0.1 with selected curve fits to the data.

in these tests were supplied by U.S. wind turbine blade manufacturers. Other specimens were constructed to systematically study the effect on fatigue properties of variations in composite structure, e.g., fiber content and reinforcement architecture. The data base contains test results that span a range of 10^3 to 5×10^8 cycles and R values of 2, 10, -1, 0.5 and 0.1. Supporting tests for ultimate tensile, ultimate compression, and modulus were also conducted for inclusion in the data base. A typical data set for uniaxial fiber lay-ups and an R value of 0.1 is shown in Figure 1.

Power Law Fit

The fiberglass composite data contained in the data base cover a wide range of properties. Mandell, et al. (1993) demonstrated that the constant amplitude, S-N fatigue data may be characterized by a power law curve fit of the form:

$$\frac{e}{e_0} = C N^{-\left(\frac{1}{m}\right)} \quad , \quad [1]$$

where e is the maximum cyclic strain if the coupon fails in tension or the minimum cyclic strain if the coupon fails in compression, e_0 is the ultimate tensile strain ϵ_{uts} or ultimate compression strain ϵ_{ucs} (for tensile and compressive failure, respectively), N is the number of cycles to failure, and m and C are the curve fitting parameters. The mean fits for uniaxial fiber lay-ups are summarized in Table I. The fits for an R value of 0.1

Table I: Power law fit of the fatigue data for uniaxial fiber lay-ups.

R	Power Law Coefficients with Range of Applicability						
	Value	1 to 10^8		10^3 to 10^8 Cycles		10^5 to 10^8 Cycles	
		C	m	C	m	C	m
0.1		1	11.3	0.969	11.6	0.740	14.3
0.5		1	15.4	0.977	16.0	0.977	16.0
-1		1	14.9	1.124	13.2	1.124	13.2
10		1	18.0	0.862	22.5	0.802	24.9
2		1	31.2	0.859	47.8	0.802	61.7

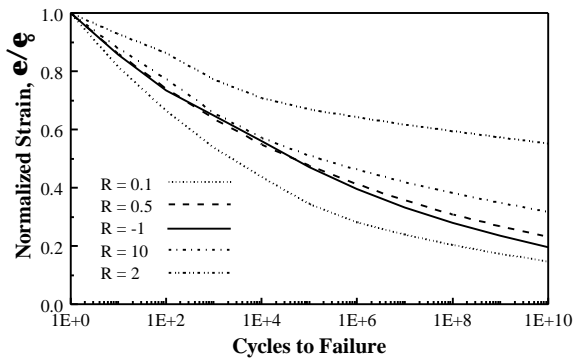


Figure 2a. Semilog plot.

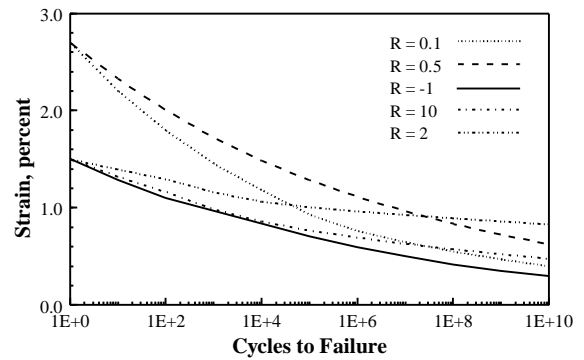


Figure 3. S-N diagram for fiberglass composites based on the MSU/DOE data base.

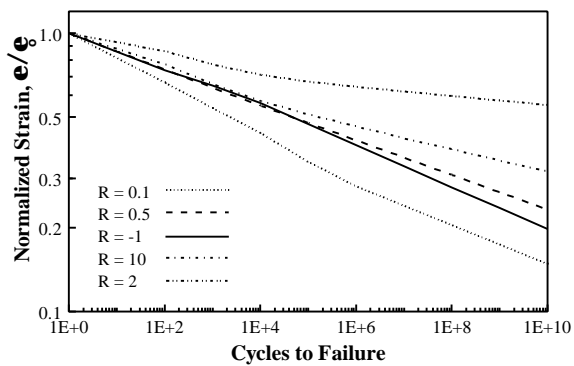


Figure 2b. Log-log plot.

Figure 2. S-N diagram for fiberglass composites normalized to failure strain.

from 10^8 to 10^{10} cycles, the power law fits are extrapolations of the 10^5 to 10^8 data.

Goodman Diagram

The data cited in the previous section describe the normalized behavior of the composites. To use this characterization in a service lifetime calculation, ϵ_o must be denormalized by the ultimate tensile (ϵ_{uts}) and compressive (ϵ_{ucs}) failure strain of the material under consideration. Typical values for industrial blade laminates are 2.7 percent and 1.5 percent, respectively [Mandell et al. 1995]. The normalized data presented in Figure 2 are scaled to these values to obtain the S-N diagram shown in Figure 3 and the Goodman diagram shown in Figure 4. In Figure 4, the plot has been normalized to ϵ_{uts} using the ratio of 2.7 to 1.5 for the tensile-to-compressive ratio.

are shown in Figure 1. In this table, the first set of parameters (labeled 1 to 10^8 cycles) is the best fit parameters when all of the S-N data and the ultimate strain are considered (the lead coefficient C has been set to one in these fits to reflect the correct ultimate strain of the material). The second set (labeled 10^3 to 10^8 cycles) is the parameters for fits to the S-N data with lifetimes that are greater than 10^3 cycles. The third set (labeled 10^5 to 10^8 cycles) is the parameters for fits to the data with lifetimes that are greater than 10^5 cycles. In the latter two sets, the value of C is not restricted to a value of one.

To obtain the “best” overall fits shown in Figure 2, the first set of parameters was used from 1 to 10^3 cycles, the second from 10^3 to 10^5 and the final from 10^5 to 10^{10} . At the intersections, an average value was used. Note that the data underlying these fits are limited to approximately 10^8 cycles. Thus,

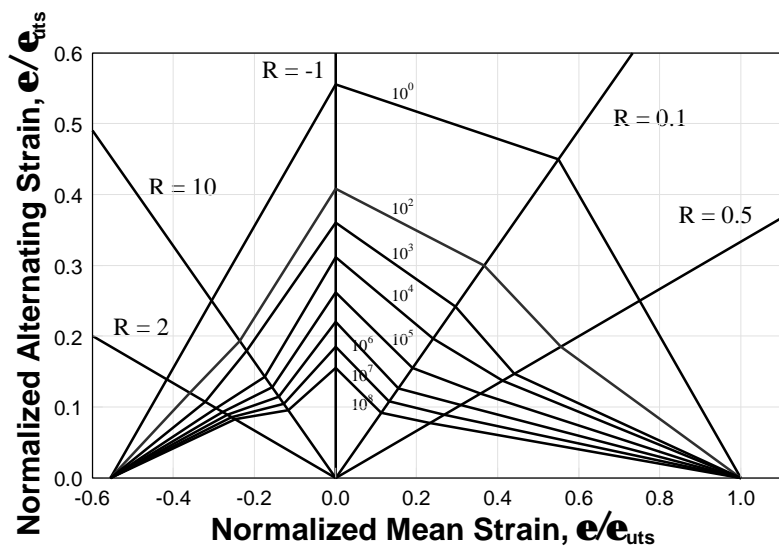


Figure 4. Normalized Goodman diagram for fiberglass composites based on the MSU/DOE data base.

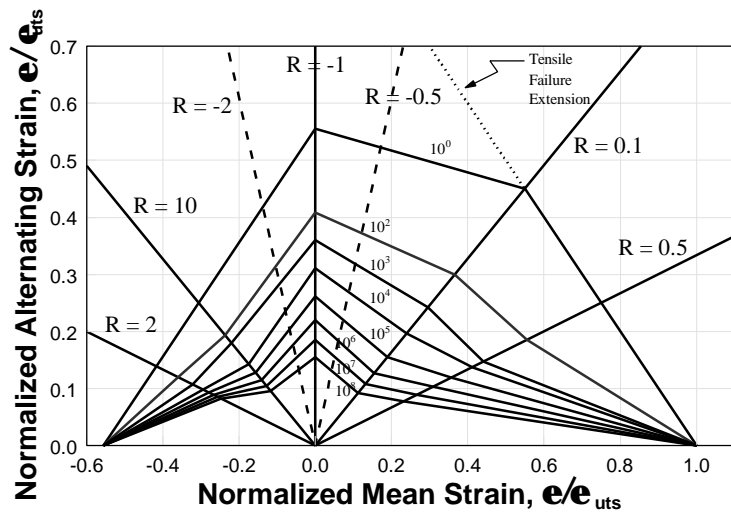


Figure 5. Goodman diagram with tensile failure extension and constant R values based on the MSU/DOE data base.

When comparing Figures 3 and 4, one notes that the Goodman diagram is based on curve fits to the ultimate tensile and compressive strains and curve fits at five R values. Between these five constant R value lines, a Goodman diagram was constructed using straight lines. This construction technique is a reasonable approximation between R values of 2, 10 and -1 and the ultimate compressive strain, and between R values of 0.1 and 0.5 and the ultimate tensile strain, because the failure mechanisms for the former are all compressive and for the latter they are all tensile. However, somewhere between an R value of -1 and 0.1, the failure mechanism changes from compressive to tensile. The transition between the two is not defined in the data base. In the rendition of the Goodman diagram shown in Figure 4, this region is also bridged with straight lines.

In Figure 5, the Goodman diagram shown in Figure 4 has been redrawn with the tensile failure extension, indicated by the dashed line, into an R range of -1 to 0.1. As shown by this extension, a tensile failure mechanism in this range will produce significantly higher strains to failure. Thus, we have chosen a conservative estimate of a Goodman diagram in this region.

In the FACT data base [DeSmet and Bach, 1994], ϵ_{uts} and ϵ_{ucs} are 2.58 percent and 1.94 percent, respectively. These values produce an almost symmetric Goodman diagram. A symmetric diagram implies that there are only small differences between tensile and compressive failures. Thus, for tensile failure (R values between 0 and 1), the MSU/DOE and the FACT data bases are in general agreement. However, for compressive failures, there are significant differences in the strain to failure, with the MSU/DOE data base predicting lower strains to failure and shorter service lifetimes. The effects of these differences on predicted service lifetimes are demonstrated below in the sample fatigue analysis.

The discrepancy in the compressive strain to failure between the two data bases may reflect a difference in the compression test

methodology. In particular, the compressive tests conducted at MSU used gauge sections with no lateral constraints, whereas, the FACT data base has a preponderance of data obtained from compression tests with lateral constraints. The in the compressive strain discrepancy can also indicate that the materials contained in the FACT data base are significantly different from those contained in the MSU/DOE data base. Until definitive tests are conducted, these differences will remain unresolved.

WISPER PROTOCOL LOAD SPECTRA

The European load spectrum (the WISPER load spectrum) was developed by an international working group composed of thirteen different European research institutes and manufacturers [Ten Have, 1992]. The objective of the effort was to specify variable-amplitude (or spectral) test-loading histories that incorporate the major features seen in the root flapwise (out-of-plane)

bending of horizontal-axis wind turbine (HAWT) blades. The European load spectrum is derived from eight load cases that are called “classes” or “modes.” The first two classes are the loads for discrete events, specifically turbine start-up (Class 1) and stopping (Class 2). The six remaining classes, 3 through 8, define the load histories for continuous operation of the turbines over their operating wind speed range. Class 3 contains representative data for mean wind speeds below 9 m/s. Classes 4 through 7 contain data for mean wind speeds of 9-11, 11-13, 13-15, and 15-17 m/s, respectively. Finally, Mode 8 describes the loads for mean wind speeds exceeding 17 m/s. Only classes 3 through 8 are used in the analyses presented here.

Kelley (1995) found that the WISPER development protocol could be successfully applied to the U.S. wind farm operating environment. He constructed a U.S. wind farm load spectrum using an operating data set that was collected from two adjacent Micon 65/13 horizontal-axis wind turbines. These turbines are located in Row 37 of a 41-row wind farm in San Geronio Pass, California. This location is near the center of a group of turbines that is characterized by low energy production and higher fatigue damage relative to other turbine locations within the wind farm. The two turbines were identical except for their rotors. One turbine had a 17-m rotor that was based on the NREL (SERI) thin-airfoil family, and the other had a 16-m rotor consisting of reconditioned, original-equipment AeroStar blades. [Tangler et al. (1990) present a complete discussion of these tests.] In all, 397 10-minute records were collected over a wide range of inflow conditions.

Kelley (1995) followed the WISPER development protocol to form the load cycle matrices for Modes 3 through 7. Data from both the NREL and AeroStar loads data were used to determine these matrices. The U.S. wind farm and the European distributions are compared with one another in Figure 6. As shown in this figure, the San Geronio (U.S. wind farm)

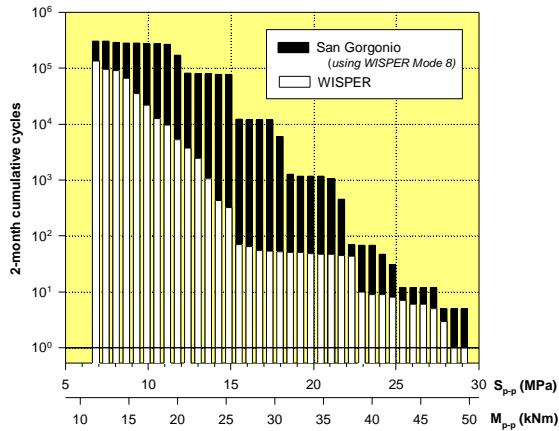


Figure 6. Cumulative 2-month reference alternating load spectra.

spectrum differs significantly from the European load spectrum (WISPER), which is based on the loads from singly-sited turbines located in relatively smooth terrain. The U.S. wind farm load spectrum contained many more and larger loading cycles than the European load spectrum. And, Sutherland and Kelly (1995) showed that the wind farm load spectrum is significantly more damaging.

Both the European and the U.S. load spectra are normalized to an amplitude range of 1 to 64, with zero load equal to 25. To convert the normalized ranges to strains requires a detailed knowledge of the design and the loads on the turbine blade. Because we are not analyzing a particular turbine blade here, we assume that the maximum nominal strain level in the blade is 0.4 percent (this strain level is commonly used in the wind industry as the maximum allowable nominal strain for the blades).

As noted above, both spectra are flap bending moment spectra. Therefore, the blade is subjected to tensile strains on one side (up wind) and compressive strains on the other (down wind). The cyclic loads on both the tensile and compressive side are considered in this analysis.

PREDICTION OF SERVICE LIFETIME

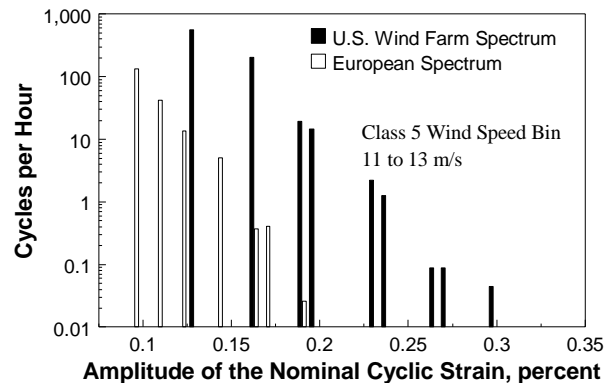
The LIFE2 analysis code for wind turbines [Sutherland and Schluter, 1989] is a PC-based, menu-driven numerical analysis package that leads a user through the steps required to characterize the loading and material properties. Miner's rule or a linear crack propagation rule is then used to calculate the time to failure. Only Miner's rule is used here.

Input Parameters

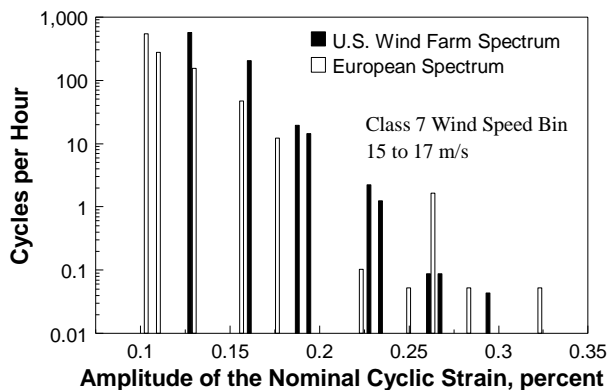
The LIFE2 code requires four sets of input variables: 1) the wind speed distribution for the turbine site as an average annual distribution, 2) the material fatigue properties, 3) a joint

distribution of mean strain and strain amplitude (or stress) for the various operational states of the turbine, and 4) a miscellaneous set of parameters that describe the operational parameters for the turbine (e.g., the cut-in and cut-out wind speed) and the stress concentration factor(s) for the turbine component. The reader is referred to Sutherland, Veers and Ashwill (1994) for a complete description of these input parameters.

For this analysis, we assume that the turbine is located at a Rayleigh site with an average wind speed of 6.3 m/s (14 mph). The fatigue properties for the MSU/DOE data base are the numerical equivalent of the data contained in the Goodman diagram shown in Figure 4. A similar numerical formulation was developed for the FACT data base by the author from the Goodman diagram developed by DeSmet and Bach (1994). Another fatigue data base, developed by Kensch (1992), was also used in the calculations. As the results of the latter two data bases are in general agreement, the analyses based on the Kensch data base are not reported here. The third input data set for the LIFE2 code is the U.S. wind farm and the European load spectra that are described above. Figures 7a and 7b present representative samples of the alternating component of the cyclic strain distribution, from class 5 and 7 wind speed bins for the



a. Strain spectra for Class 5 Wind Speed Bin.



b. Strain spectra for Class 7 Wind Speed Bin.

Figure 7. Typical load spectra.

Table II. Predicted service lifetime in years.

Bending Direction	U.S. Wind Farm Spectrum		European Spectrum	
	MSU/DOE	FACT	MSU/DOE	FACT
Tensile	44.9	67.5	186.	618.
Compressive	23.5	136.	90.0	1130

European and the U.S. wind farm data bases. Complete descriptions of these distributions are given by Kelley (1995). The fourth and final input set describes the operation of the turbine and the stress concentration factor. For these calculations, the turbine is assumed to operate between 5.4 m/s (12 mph) and 25 m/s (56 mph). The stress concentration factor is assumed to be 2.5.

Damage Calculations

The input parameters described above were used in the LIFE2 code to predict service lifetimes. The results of these analyses are summarized in Table II.

First, the predicted service lifetimes in Table II illustrate that the WISPER load spectrum from northern European sites (the European spectrum) significantly underestimates the WISPER protocol load spectrum from a U.S. wind farm site (the U.S. wind farm spectrum); i.e., the WISPER protocol overestimates the service lifetime at this U.S. site. And, second, Table II illustrates that the MSU/DOE data base predicts the blade will fail in compression and at shorter lifetimes than predicted by the FACT data base.

Comparison of the Spectral Loads: As shown in Figure 6 and analyzed by Kelley (1995) and Sutherland and Kelley (1995), the WISPER load spectrum for U.S. wind farms contains many more cycles than does the European spectrum, and the wind farm spectrum is more damaging. The latter conclusion is illustrated in Table II by comparing the predicted lifetimes in the first column to the third column and the second to the fourth. In all cases, the European load spectrum significantly overestimates the service lifetime at the U.S. wind farm site.

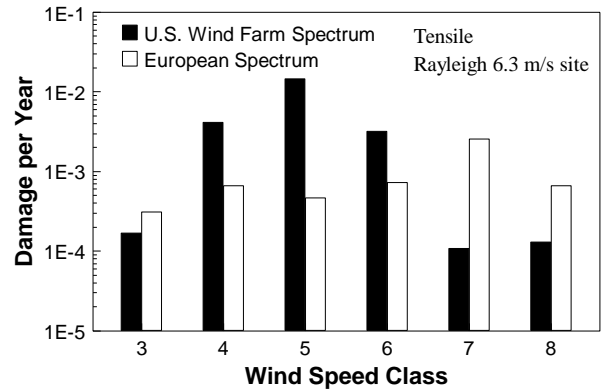
A more detailed comparison of the damage is shown in Figure 8. In this figure we examine the damage \mathcal{D} associated with each load spectrum. The damage at strain ϵ_i is defined by Miner's Rule to be

$$\mathcal{D}(\epsilon_i) = \frac{n[(\epsilon_i)_a, (\epsilon_i)_m]}{N[(\epsilon_i)_a, (\epsilon_i)_m]}, \quad [2]$$

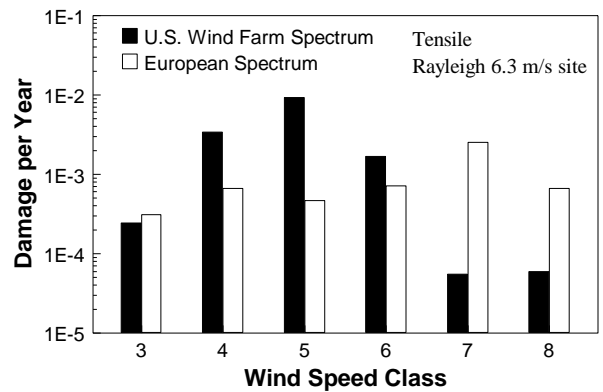
where n is the number of cycles in the spectrum at alternating strain $(\epsilon_i)_a$, mean strain $(\epsilon_i)_m$ and N is the number of cycles to failure at the same strain level. The total damage is simply the sum of the damage over all strain cycles in the spectrum. By Miner's Rule, failure occurs when the total damage accumulates to one, or inversely, when the damage is summed over all stress

cycles in time t , the service lifetime of the component is equal to the reciprocal of the damage.

As shown in Figure 8, the damage is concentrated in the mid-range wind speed bins (i.e., wind speed classes 4, 5 and 6) for the U.S. wind farm spectrum and in the upper wind speed bins (i.e., wind speed classes 7 and 8) for the European load spectrum. This result could be anticipated by a close examination of Figure 7. As shown in Figure 7a, the strain cycles in Class 5 for the U.S. wind farm spectrum have more



a. MSU/DOE fatigue data base.



b. FACT data base.

Figure 8. The damage spectra for the two fatigue data bases by wind speed bin.

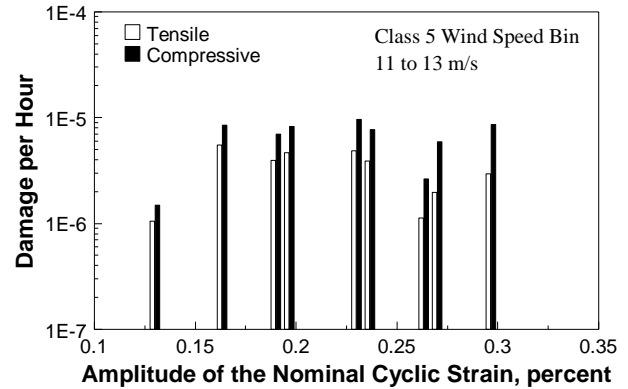
cycles at higher amplitudes than the European spectrum. Figure 7b, illustrates that in Class 7, the distributions are reversed, with the European spectrum containing more cycles at higher amplitudes. Again, when the damage for all wind speed classes are totaled, the European spectrum is less damaging than the U.S. wind farm spectrum.

One must be careful in drawing general conclusions from these observations. These analyses are based on a limited set of data from two almost identical turbines located at a single, U.S. wind farm site. Their limited nature precludes us from determining if this “U.S. wind farm spectrum” is representative of the load spectra on other turbines in different wind farms. Also, one should remember that the WISPER spectrum was never intended to duplicate the actual load spectrum on a turbine blade. This spectrum is a fatigue test loading standard based on variable amplitude load cycles for flap bending of HAWT blades on multiple turbines.

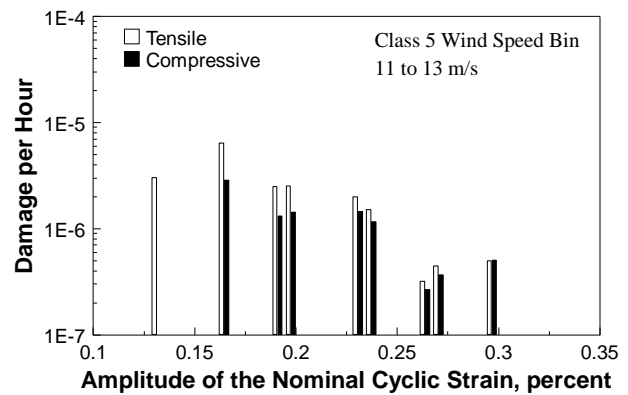
Comparison of Material Data Bases: The predicted service lifetimes shown in Table II illustrate that the MSU/DOE data base predicts, for both the U.S. and the European load spectra, that the blade will fail in compression and at shorter lifetimes than predicted by the FACT data base. These observations are drawn by comparing the first column to the second and the third to the fourth. The prediction of compressive failure is due to the asymmetry in the Goodman diagram of the MSU/DOE database, and the prediction of shorter lifetimes is due to the higher ultimate strains measured for the materials contained in the FACT data base.

To examine the asymmetry in greater detail, we will examine the damage rate (see Equation 2) produced by the U.S. wind farm strain spectrum in wind speed class 5 that is discussed above and shown in Figure 7a. The damage associated with these strain cycles is shown in Figures 9.

As illustrated in Figure 9a and in Table II, compressive strains produce significantly more damage than equivalent tensile loads when the MSU/DOE data base is used to determine the damage. This result is directly related to the strong asymmetry between compression and tension failures in the MSU/DOE data base that is characterized by the Goodman diagram shown in Figure 4. Consider the component of the strain distribution in the class 5 wind speed bin, shown in Figure 7a, that is located near a nominal alternating strain amplitude of 0.3 percent. This component has a rate of accumulation of approximately 0.045 cycles per hour and nominal amplitude of 0.3 percent strain and a nominal mean of 0.1 percent strain. For tensile bending with a stress concentration factor of 2.5, this converts to 1.0 percent maximum strain and -0.5 percent minimum strain. For compressive bending, this converts to 0.5 percent maximum strain and -1.0 percent minimum strain. Thus, R equals -0.5 for tension and -2 for compression. As shown in the Goodman diagram in Figure 5, the tensile failure strains to failure (see the R equal -0.5 dashed line in the Figure) are higher than the compressive failure strains (R equal -2 dashed line) for most alternating strains. This observation translates to a lower service lifetime in compression.



a. Damage spectra using the MSU/DOE data base.



b. Damage spectra using the FACT data base.

Figure 9. Typical tensile and compressive damage spectra for the class 5 wind speed bin.

Likewise, as illustrated in Figure 9b and in Table II, tensile strains produce significantly more damage than equivalent compressive loads when the FACT data base is used to determine the damage. This result is attributed to the approximately symmetric Goodman diagram in the FACT data base.

As one may deduce from the predicted service lifetimes in Table II, similar results are obtained for the European load spectrum.

CONCLUDING COMMENTS

The MSU/DOE data base contains over 2200 data points with test results for fiberglass composites with polyester, vinyl ester and epoxy matrices and with a variety of fiber contents. These data may be characterized by a power law curve fit when normalized to their ultimate tensile and compression failure strains. The Goodman diagram constructed from these data displays a significant asymmetry between the tensile and compressive failure zones. A similar diagram constructed from the FACT data base does not display a pronounced asymmetry.

The fatigue calculations demonstrate the significance of these differences in the Goodman diagrams for the MSU/DOE and the FACT fatigue data bases. For both load spectra used in this example, the data bases predict similar lifetimes in tension, but in compression, the data bases predict very different lifetimes. The FACT data base predicts the critical failure mode to be tensile, and the MSU/DOE data base predicts the critical mode to be compressive. As discussed in detail above, these differences are a direct result of the asymmetric MSU/DOE Goodman diagram and the approximately symmetric FACT Goodman diagram. We hypothesize that the differences may be attributed to testing methods (lateral constraints). However, these differences could also indicate that the materials contained in the FACT data base are significantly different from those contained in the MSU/DOE data base. Until definitive tests are conducted, these differences will remain unresolved.

The analyses presented here further illustrate that the European load spectrum from northern European sites (the WISPER load spectrum) significantly underestimates a U.S. wind farm load spectrum (the WISPER protocol load spectrum derived from wind turbine loads data at a U.S. wind farm site); i.e., the European load spectrum significantly underestimates the number and magnitude of the loads observed at a U.S. wind farm site. Significantly more fatigue damage is occurring at the U.S. site because the inflow in the wind farm environment produces more cycles and higher loads in the turbine. Thus, there are fundamental differences in the two service environments.

ACKNOWLEDGMENTS

This work is supported by the U.S. Department of Energy under contract DE-AC04-94AL85000.

The author wishes to extend special acknowledgments to Neil Kelley and John Mandell. As cited in the paper, the author has drawn heavily upon their work for the data and the analyses presented in this paper.

REFERENCES

- Creed, R.F., Jr., 1993, *High Cycle Tensile Fatigue of Unidirectional Fiberglass Composite Tested at High Frequency*, M.S. Thesis, Dept. of Chemical Engineering, Montana State University, Bozeman.
- DeSmet, B.J. and P.W. Bach, 1994, *DATABASE FACT: Fatigue of Composites for Wind Turbines*, ECN-C--94-045, ECN, Petten, the Netherlands.
- Kelley, N.D., 1995, "A Comparison of Measured Wind Park Load Histories With The WISPER and WISPERX Load Spectra," *Wind Energy 1995*, SED-Vol. 16, ASME, p. 107.
- Kensche, C.W., 1992, *High Cycle Fatigue of Glass Fibre Reinforced Epoxy Materials for Wind Turbines*, DLR-FB 92-17, DLR, Stuttgart.
- Mandell, J.F., Sutherland, H.J., Creed, R.J., Jr., Belinky, A.J., and Wei, G., 1995, "High Cycle Tensile and Compressive Fatigue of Glass Fiber-Dominated Composites," *ASTM, Sixth Symposium on Composites: Fatigue and Fracture*, in publication.
- Mandell, J.F., Creed, R.J., Jr., Pan, Q., Combs, D.W., and Shrinivas, M., 1994, "Fatigue of Fiberglass Generic Materials and Substructures," *Wind Energy 1994*, SED-Vol. 15, ASME, p. 207.
- Mandell, J.F., Reed, R.M., Samborsky, D.D., and Pan, Q., 1993, "Fatigue Performance of Wind Turbine Blade Composite Materials," *Wind Energy 1993*, SED-Vol. 14, ASME, p. 191.
- Mandell, J.F., Reed, R.M., and Samborsky, D.D., 1992, *Fatigue of Fiberglass Wind Turbine Materials*, SAND92-7005, Sandia National Laboratories, Albuquerque.
- Samborsky, D.D., and Mandell, J.F., 1996, "Fatigue Resistant Fiberglass Laminates for Wind Turbine Blades," *Wind Energy 1996*, ASME, in publication.
- Sutherland, H.J., and Kelley, N.D., 1995, "Fatigue Damage Estimate Comparisons for Northern European and U.S. Wind Farm Loading Environments," *Proceedings of WindPower '95*, AWEA, Washington, DC.
- Sutherland, H.J., and Mandell, J.F., 1996, "Application of the U.S. High Cycle Fatigue Data Base to Wind Turbine Blade Lifetime Predictions," *Wind Energy 1996*, ASME, in publication.
- Sutherland, H.J., and Schluter, L.L., 1989, "The LIFE2 Computer Code - Numerical Formulation and Input Parameters," *Proc. WindPower '89*, SERI/TP-257-3628, American Wind Energy Association, Washington, DC.
- Sutherland, H.J., Veers, P.S., and Ashwill, T.D., 1994, "Fatigue Life Prediction for Wind Turbines: A Case Study on Loading Spectra and Parameter Sensitivity," *Case Studies for Fatigue Education*, ASTM STP 1250, p. 174.
- Tangler, J., Smith B., Jager D., and Olsen, T., 1990, *Atmospheric Performance of the SERI Thin-Airfoil Family*, SERI/TP-257-3939, Solar Energy Research Institute, Golden, CO.
- Ten Have, A.A., 1992, *WISPER and WISPERX: Final Definition of Two Standardized Fatigue Loading Sequences for Wind Turbine Blades*, NLR-TP-91476U, National Aerospace Laboratory NLR, Amsterdam, the Netherlands.